International Journal of Advanced Engineering and Management Research
Vol. 3 Issue 5; 2018

www.ijaemr.com ISSN: 2456-3676

ANALYSIS OF WELD MOLTEN METAL KINEMATIC VISCOSITY OF TIG MILD STEEL WELD

Anowa, H.D, Achebo, J.I, Ozigagun .A and Etin-osa, E.C
Department of Production Engineering, University of Benin, Benin City, Nigeria
Email address:
dorothyanowa@yahoo.com (Anowa, H.D); josephachebo@yahoo.co.uk (Achebo, J.I),
andrewzigs@yahoo.com and etinosa.eruogun@uniben.edu (Etin-osa, E.C))

Abstract

Viscosity is an important property of liquid metals during welding because it controls the rate of transport of liquid metals, which may lead to weld defects such as cracks, porosity etc., which greatly affects weld quality. This study was carried out with the aim of optimizing and predicting the weld molten metal fluidity of weldment. Mild steel plate was cut into dimension 60mmx40mmx10mm with a power hacksaw, grinded and cleaned before the welding process. The experimental matrix was made of twenty (20) runs, generated by the design expert 7.01 software adopting the central composite design. The result obtained in this research study shows that a high viscosity produces weldment with better structural integrity. The model produced numerical optimal solution of current 150 amps, voltage of 20 volts and gas flow rate of 17l/min will produce a welded structure having kinematic viscosity of 1.179m2/s at a desirability value of 94.6%.

Introduction

Hildebrand and Lamoreaux (1976) defined fluidity as the reciprocal of viscosity. Korolezuk-hejnak and Migas (2012) and Bakhtiyarov and Over felt (1999) described viscosity as a rheological property of materials which presents itself when the velocity gradient between neighbouring layers of material is deserved. These authors saw viscosity as an important rheological parameter for understanding the hydrodynamics and kinetics of reactions in metal refining, casting, metal and slag tapping or dripping. For instance, the rate of the rise of gas bubbles and non-metallic inclusions through a molten metal is primarily related to viscosity Di Sabatino et al. (2008) and Moran do et al. (2015). Also, the kinetics of reactions between metal and slag can be monitored by continuous measurements of the liquid's viscosity. Kaptay (2005) said that the viscosity of liquid metals and alloys is one of the technologically important transport properties needed to develop and optimize metallurgical technologies. Boda et al (2015) were of the opinion that viscosity of a fluid is a measure of its resistance to gradual deformation by shear stress or tensile stress. The authors said that viscosity is a property arising from collisions between neigh boring particles in a fluid that are moving at different velocities Davies (1992). When the fluid is forced by the force of the shielding gas and arc temperature, the particles which comprises the fluid generally move more quickly near the weld pool axis (center) and more slowly near the walls of the work piece (liquid-solid interface). Therefore these forces are needed to overcome the friction between particle layers and keep the fluid moving (detaching). If any two layers of liquid move with different velocities, the top layer moves faster than the next layer due to viscous drag. It is therefore observed that the kinematic viscosity of all liquids decreases as temperature of liquids increases and vice versa.

Ritwik (2012) wrote that rheology describes the deformation and flow behaviour in all types of matter. Deformation is the process of changing the relative position of the various parts in a body. Upon deformation, spontaneous return to the undeformed shape is called elasticity, whereas an irreversible change leading to dissipation of the mechanical energy as heat is termed 'flow'. To create flow, a stress must be applied. Under an applied stress (i.e. shielding gas and arc temperature, in terms of welding) the type of deformation that occurs is known as shear. Simple shear can be visualised as a set of infinitely thin parallel plates sliding over one another as in a deck of cards. Since each plane is reluctant to move with respect to the other, there is a resistance to flow. This resistance is what is now referred to as viscosity. Due to the similarity between the frictional forces in solids, which resists the motion of one solid over another, and the resistance to flow in fluids sometimes referred to as internal friction, viscosity creates a picture in the internal friction between the different layers fluid Achebo (2012).

Materials and Methods

Materials

100 pieces of mild steel coupons measuring 80 x 40 x10 was used for the experiments, the experiment was performed 20 times using 5 specimens for each run. The key parameters considered in this work are welding current, welding speed, gas flow rate, and welding voltage. The range of the process parameters obtained from literature which is shown in the table 1. The tungsten inert gas welding equipment was used to weld the plates after the edges have been bevelled and machined. Figure 1 shows the TIG welding setup. The welding process uses a shielding gas to protect the weld specimen from atmospheric interaction, 100% pure Argon gas was used in this research study. Figure 2 shows the shielding gas cylinder and regulator. Figure 3 shows the weld sample

Figure 1: TIG equipment

Figure 2: shielding gas cylinder and regulator

Table 1: Process parameters and their levels

Factors	Unit	Symbol	Low (-1)	High (+1)
Welding Current	Ampere	I	130	170
Welding Voltage	Volts	V	20	24
Gas Flow Rate	Lit/min	GFR	13	17

Figure 3 weld samples

Method of Data Collection

The central composite design matrix was developed using the design expert software, producing 20 experimental runs. The input parameters and output parameters make up the experimental matrix and the responses recorded from the weld samples was used as the data. The data matrix is determined by the number of input parameters which is expressed in the equation 2n +2n +k, where k is number of center points,2n is the number of axial points and 2nis the number of factorial points.

The matrix can be expressed in actual values which fall within the range stated, is presented in figure 4

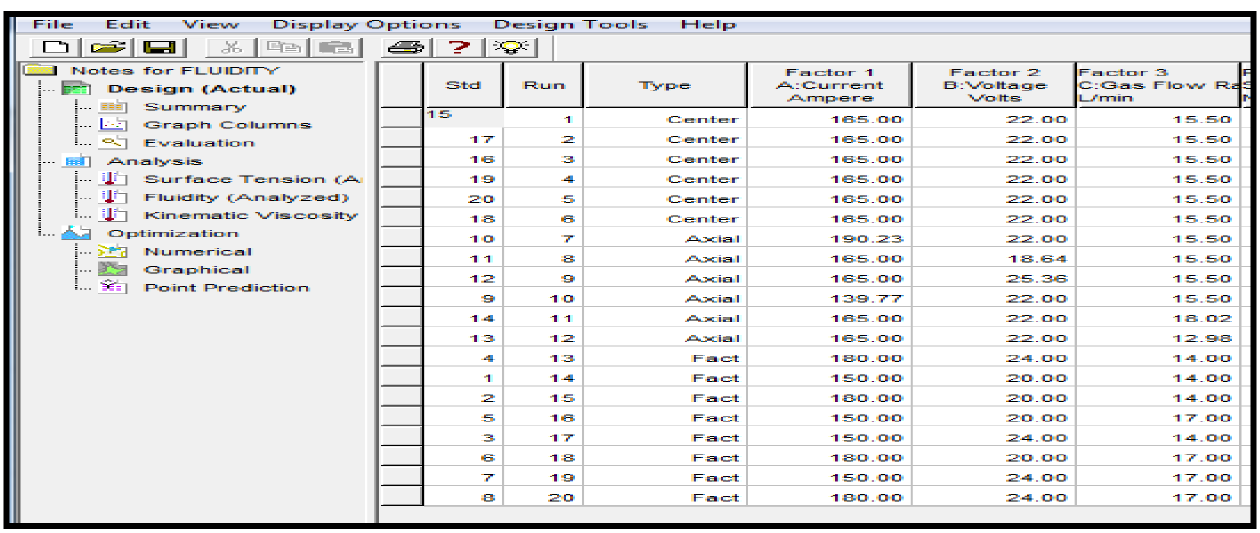

Std	Run	Type	Factor 1 A:Current Ampere	Factor 2 B:Voltage Volts	Factor 3 C:Gas Flow Ra L/min
15	1	Center	165.00	22.00	15.50
17	2	Center	165.00	22.00	15.50
16	3	Center	165.00	22.00	15.50
19	4	Center	165.00	22.00	15.50
20	5	Center	165.00	22.00	15.50
18	6	Center	165.00	22.00	15.50
10	7	Axial	190.23	22.00	15.50
11	8	Axial	165.00	18.64	15.50
12	9	Axial	165.00	25.36	15.50
9	10	Axial	139.77	22.00	15.50
14	11	Axial	165.00	22.00	18.02
13	12	Axial	165.00	22.00	12.98
4	13	Fact	180.00	24.00	14.00
1	14	Fact	150.00	20.00	14.00
2	15	Fact	180.00	20.00	14.00
5	16	Fact	150.00	20.00	17.00
3	17	Fact	150.00	24.00	14.00
6	18	Fact	180.00	20.00	17.00
7	19	Fact	150.00	24.00	17.00
8	20	Fact	180.00	24.00	17.00

Figure 4: Central Composite Design Matrix (CCD) in actual values

Model Validation for ANOVA

i) Coefficient of determination R^2

The coefficient of determination R^2 was used to validate the developed model equation 1 shows the expression for the diagnostic tool. The model targetispredicted using the R^2.

$$R^2 = \frac{\sum_{i=1}^{n}(y_i - \hat{y}_i)^2}{\sum_{i=1}^{n}(y_i - \hat{y}_i)^2} \quad (1)$$

The experimental observation is represented with . is the fitted observation.

is the average observation

$R^2 \leq 1$ (R^2 is less than or equal to one in most cases)

ii) The adjusted coefficient determination is determined and used to validate the developed model.

It is expressed in equation 2.

$$AdjR^2 = \frac{\sum (y_i - \hat{y}_i) / n-k}{\sum (y_i - \bar{y}) / n-1} \quad (2)$$

When n is the input process parameters, K is the no of responses and the observation for the experiment is represented with yi and y is fitted observation with y as the average observation. R^2 value is always below 1 (Ibrahim IBN, 2009).

RESULTS AND DISCUSSION

The design matrix showing the real value of three input variables namely; current (Amp), voltage (volts) and gas flow rate (L/min) and three responses namely; (surface tension, fluidity and kinematic viscosity) is presented in Figure 5

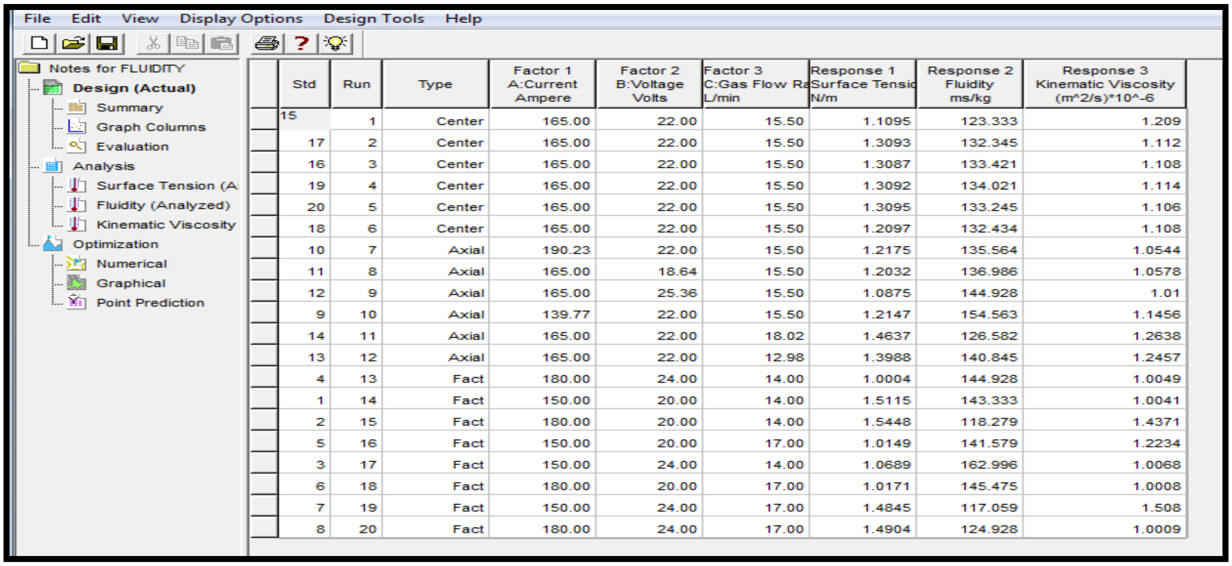

Std	Run	Type	Factor 1 A:Current Ampere	Factor 2 B:Voltage Volts	Factor 3 C:Gas Flow Ra L/min	Response 1 Surface Tensio N/m	Response 2 Fluidity ms/kg	Response 3 Kinematic Viscosity (m^2/s)*10^-6
15	1	Center	165.00	22.00	15.50	1.1095	123.333	1.209
17	2	Center	165.00	22.00	15.50	1.3093	132.345	1.112
16	3	Center	165.00	22.00	15.50	1.3087	133.421	1.108
19	4	Center	165.00	22.00	15.50	1.3092	134.021	1.114
20	5	Center	165.00	22.00	15.50	1.3095	133.245	1.106
18	6	Center	165.00	22.00	15.50	1.2097	132.434	1.108
10	7	Axial	190.23	22.00	15.50	1.2175	135.564	1.0544
11	8	Axial	165.00	18.64	15.50	1.2032	136.986	1.0578
12	9	Axial	165.00	25.36	15.50	1.0875	144.928	1.01
9	10	Axial	139.77	22.00	15.50	1.2147	154.563	1.1456
14	11	Axial	165.00	22.00	18.02	1.4637	126.582	1.2638
13	12	Axial	165.00	22.00	12.98	1.3988	140.845	1.2457
4	13	Fact	180.00	24.00	14.00	1.0004	144.928	1.0049
1	14	Fact	150.00	20.00	14.00	1.5115	143.333	1.0041
2	15	Fact	180.00	20.00	14.00	1.5448	118.279	1.4371
5	16	Fact	150.00	20.00	17.00	1.0149	141.579	1.2234
3	17	Fact	150.00	24.00	14.00	1.0689	162.996	1.0068
6	18	Fact	180.00	20.00	17.00	1.0171	145.475	1.0008
7	19	Fact	150.00	24.00	17.00	1.4845	117.059	1.508
8	20	Fact	180.00	24.00	17.00	1.4904	124.928	1.0009

Figure 5: Design matrix showing the real values and the experimental values

The model summary which shows the factors and their lowest and highest values including the mean and standard deviation is presented as shown in Table 6; Result of Table 6 revealed that the model is of the quadratic type which requires the polynomial analysis order as depicted by a typical response surface design. The minimum value of kinematic viscosity was observed to be $1.001x10^{-6}m^2/s$, the maximum value was observed to be $1.508x10^{-6}m^2/s$, with a mean value of $1.136x10^{-6}$and standard deviation of $0.140x10^{-6}$.

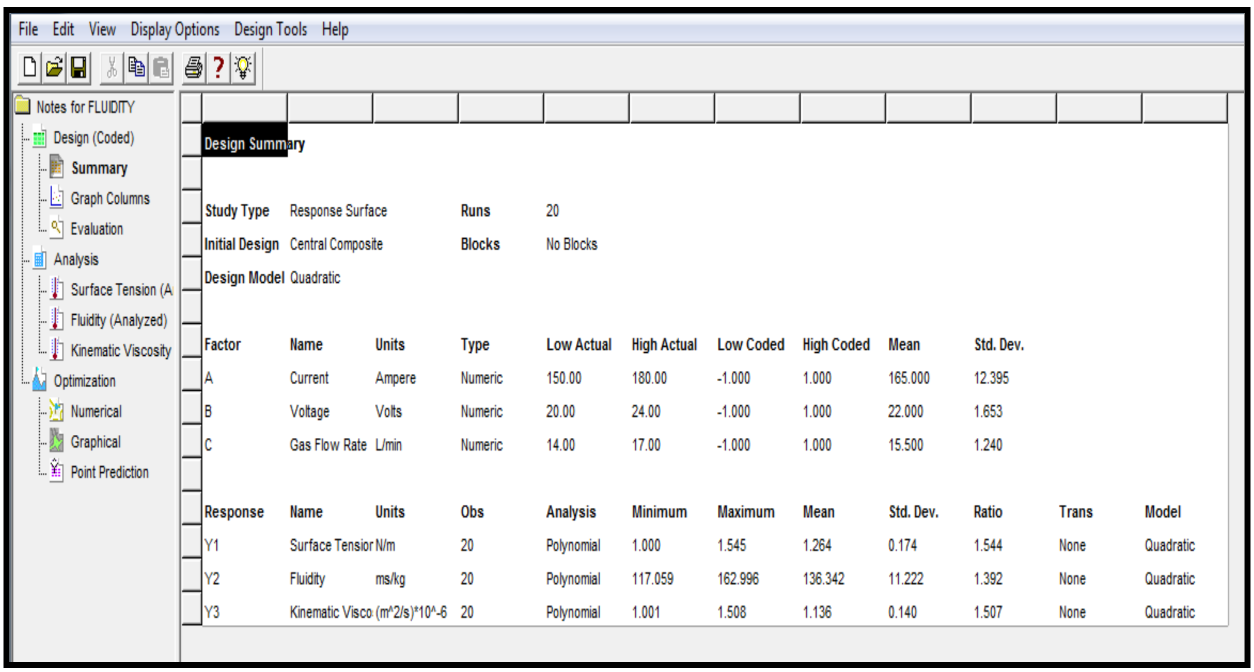

Study Type	Response Surface		Runs	20							
Initial Design	Central Composite		Blocks	No Blocks							
Design Model	Quadratic										
Factor	Name	Units	Type	Low Actual	High Actual	Low Coded	High Coded	Mean	Std. Dev.		
A	Current	Ampere	Numeric	150.00	180.00	-1.000	1.000	165.000	12.395		
B	Voltage	Volts	Numeric	20.00	24.00	-1.000	1.000	22.000	1.653		
C	Gas Flow Rate	L/min	Numeric	14.00	17.00	-1.000	1.000	15.500	1.240		
Response	Name	Units	Obs	Analysis	Minimum	Maximum	Mean	Std. Dev.	Ratio	Trans	Model
Y1	Surface Tensior	N/m	20	Polynomial	1.000	1.545	1.264	0.174	1.544	None	Quadratic
Y2	Fluidity	ms/kg	20	Polynomial	117.059	162.996	136.342	11.222	1.392	None	Quadratic
Y3	Kinematic Visco	(m^2/s)*10^-6	20	Polynomial	1.001	1.508	1.136	0.140	1.507	None	Quadratic

Figure 6: RSM design summary

To validate the suitability of the quadratic model in analyzing the experimental data, the sequential model sum of squares were calculated for kinematic viscosity as presented in figure 7

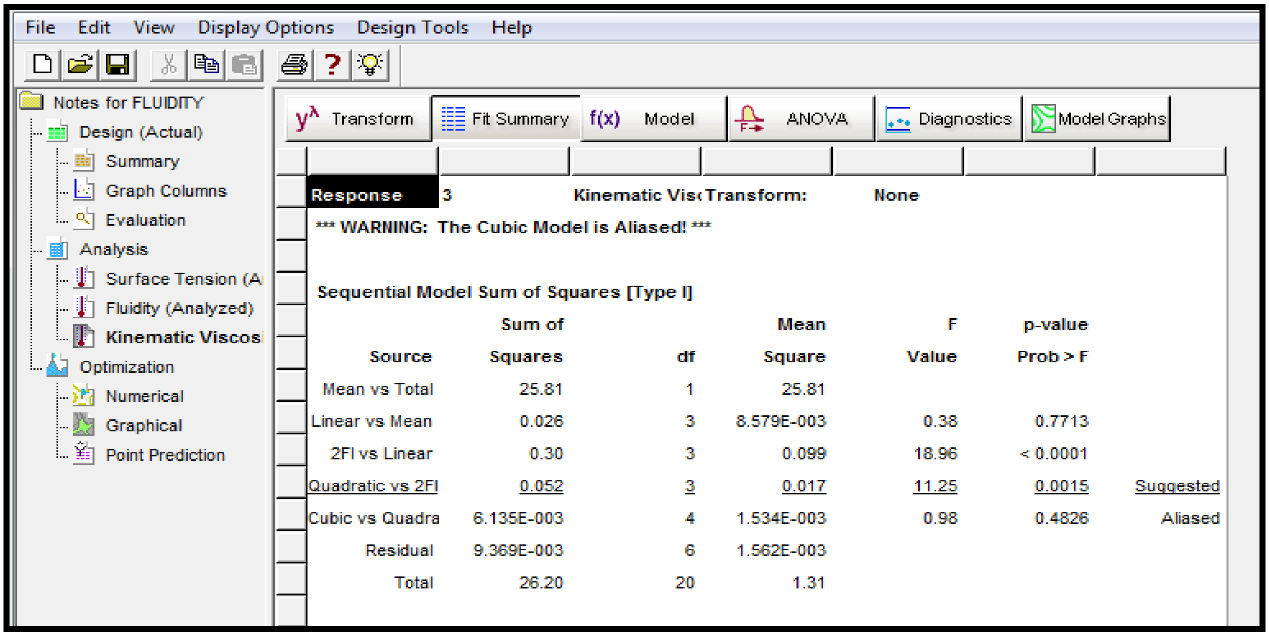

Response 3 Kinematic Visc Transform: None

*** WARNING: The Cubic Model is Aliased! ***

Sequential Model Sum of Squares [Type I]

Source	Sum of Squares	df	Mean Square	F Value	p-value Prob > F	
Mean vs Total	25.81	1	25.81			
Linear vs Mean	0.026	3	8.579E-003	0.38	0.7713	
2FI vs Linear	0.30	3	0.099	18.96	< 0.0001	
Quadratic vs 2FI	0.052	3	0.017	11.25	0.0015	Suggested
Cubic vs Quadra	6.135E-003	4	1.534E-003	0.98	0.4826	Aliased
Residual	9.369E-003	6	1.562E-003			
Total	26.20	20	1.31			

Figure 7: Sequential model sum of square for kinematic viscosity

The sequential model sum of squares table shows the accumulating improvement in the model fit as terms are added. Based on the calculated sequential model sum of square, the highest order polynomial where the additional terms are significant and the model is not aliased was selected as the best fit. From the results of figure 7 it was observed that the cubic polynomial was aliased hence cannot be employed to fit the final model. In addition, the quadratic and 2FI model were suggesed as the best fit thus justifying the use of quadratic polynomial in this analysis

To test how well the quadratic model can explain the underlying variation associated with the experimental data, the lack of fit test was estimated for kinematic viscosity. Model with significant lack of fit cannot be employed for prediction. Results of the computed lack of fit is presented in Figure 8.

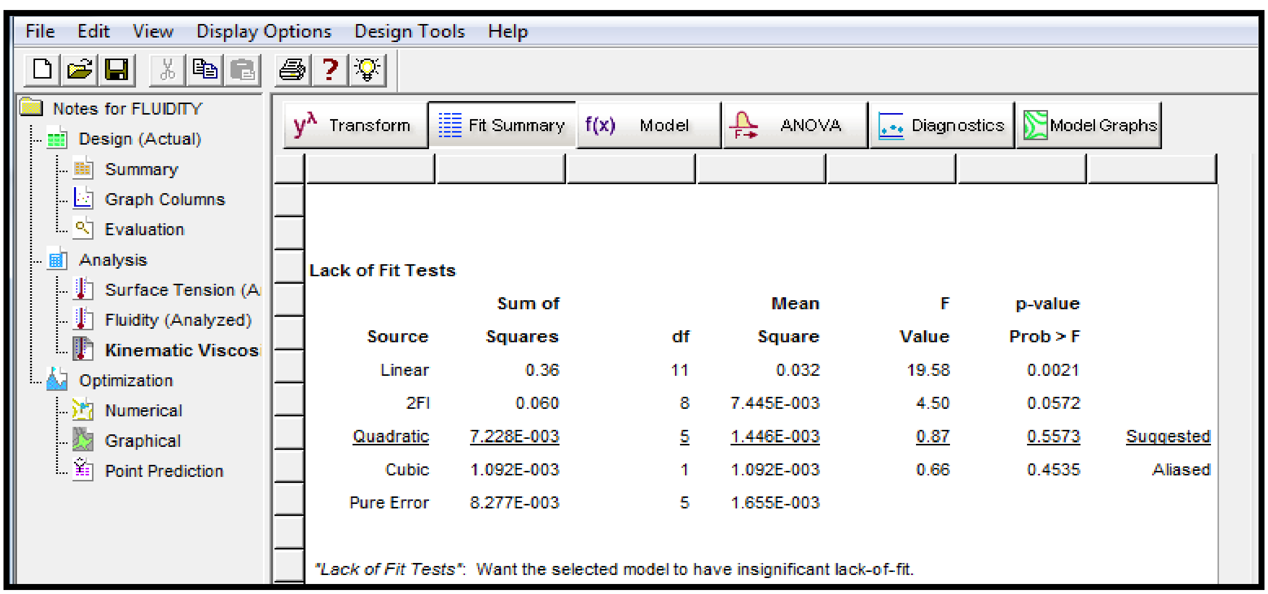

Lack of Fit Tests

Source	Sum of Squares	df	Mean Square	F Value	p-value Prob > F	
Linear	0.36	11	0.032	19.58	0.0021	
2FI	0.060	8	7.445E-003	4.50	0.0572	
Quadratic	7.228E-003	5	1.446E-003	0.87	0.5573	Suggested
Cubic	1.092E-003	1	1.092E-003	0.66	0.4535	Aliased
Pure Error	8.277E-003	5	1.655E-003			

"Lack of Fit Tests": Want the selected model to have insignificant lack-of-fit.

Figure 8: Lack of fit test for kinematic viscosity

The model summary statistics computed for kinematic viscosity is presented in figure9

Model Summary Statistics

Source	Std. Dev.	R-Squared	Adjusted R-Squared	Predicted R-Squared	PRESS	
Linear	0.15	0.0659	-0.1092	-0.7252	0.67	
2FI	0.072	0.8263	0.7461	0.6168	0.15	
Quadratic	0.039	0.9603	0.9246	0.8176	0.071	Suggested
Cubic	0.040	0.9760	0.9240	0.3528	0.25	Aliased

"Model Summary Statistics": Focus on the model maximizing the "Adjusted R-Squared" and the "Predicted R-Squared".

Figure 9: Model summary statistics for kinemstic viscosity

Analysis of the model standard error was employed to assess the suitability of response surface methodology using the quadratic model to minimize the surface tension, maximize the fluidity and maximize the kinematic viscosity. The computed standard errors for the selected responses are presented in figure 10.

File Edit View Display Options Design Tools Help

Notes for FLUIDITY
Design (Coded)
Summary
Graph Columns
Evaluation
Analysis
Surface Tension (A
Fluidity (Analyzed)
Kinematic Viscosity
Optimization
Numerical
Graphical
Point Prediction

f(x) Model | Results | Graphs

Term	StdErr**	VIF	Ri-Squared	Power at 5 % alpha level for effect of 0.5 Std. Dev.	1 Std. Dev.	2 Std. Dev.
A	0.27	1.00	0.0000	13.3 %	38.6 %	91.4 %
B	0.27	1.00	0.0000	13.3 %	38.6 %	91.4 %
C	0.27	1.00	0.0000	13.3 %	38.6 %	91.4 %
AB	0.35	1.00	0.0000	9.8 %	24.9 %	72.2 %
AC	0.35	1.00	0.0000	9.8 %	24.9 %	72.2 %
BC	0.35	1.00	0.0000	9.8 %	24.9 %	72.2 %
A^2	0.26	1.02	0.0179	40.4 %	92.7 %	99.9 %
B^2	0.26	1.02	0.0179	40.4 %	92.7 %	99.9 %
C^2	0.26	1.02	0.0179	40.4 %	92.7 %	99.9 %

**Basis Std. Dev. = 1.0

Figure 10: Result of computed standard errors

From the results of figure 10, it was observed that the model possess a low standard error ranging from 0.27 for the individual terms, 0.35 for the combine effects and 0.26 for the quadratic terms. Standard errors should be similar within type of coefficient; smaller is better. The error values were also observed to be less than the model basic standard deviation of 1.0 which suggests that response surface methodology was ideal for the optimization process. Variance inflation factor (VIF) of approximately 1.0 as observed in Table 10 was good since ideal VIF is 1.0. VIF's above 10 are cause for alarm, indicating coefficients are poorly estimated due to multicollinearity. In addition, the Ri-squared value was observed to be between 0.0000 to 0.0179 which is good. High Ri-squared (above 1.0) means that design terms are correlated with each other, possibly leading to poor models. The correlation matrix of regression coefficient is presented in figure 11

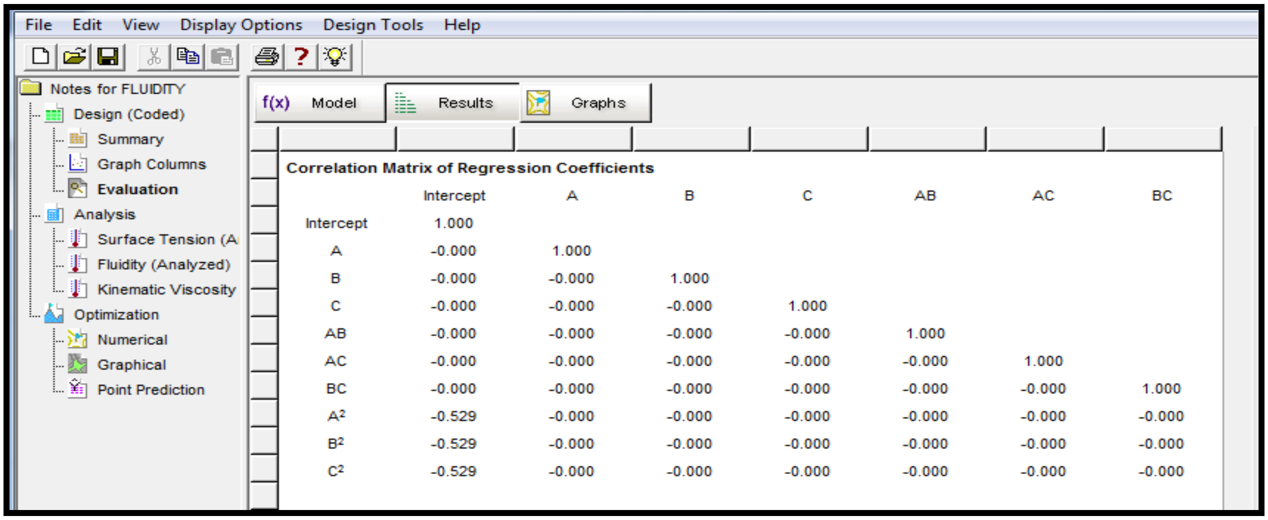

Correlation Matrix of Regression Coefficients

	Intercept	A	B	C	AB	AC	BC
Intercept	1.000						
A	-0.000	1.000					
B	-0.000	-0.000	1.000				
C	-0.000	-0.000	-0.000	1.000			
AB	-0.000	-0.000	-0.000	-0.000	1.000		
AC	-0.000	-0.000	-0.000	-0.000	-0.000	1.000	
BC	-0.000	-0.000	-0.000	-0.000	-0.000	-0.000	1.000
A^2	-0.529	-0.000	-0.000	-0.000	-0.000	-0.000	-0.000
B^2	-0.529	-0.000	-0.000	-0.000	-0.000	-0.000	-0.000
C^2	-0.529	-0.000	-0.000	-0.000	-0.000	-0.000	-0.000

Figure 11: Correlation matrix of regression coefficients

Lower values of the off diagonal matrix as observed in Table 11 indicates a well fitted model that is strong enough to navigate the design space and adequately optimize the selected response variables. From the results of figure 11, it was observed that the off diagonal matrix had coefficients that were approximately 0.00 which is an indication that the quadratic model was the ideal one for this analysis since off diagonal matrix greater than 0.00 is cause for alarm indicating a model having coefficients that are poorly correlated.

To understand the influence of the individual design points on the model's predicted value, the model leverages were computed as presented in figure 12

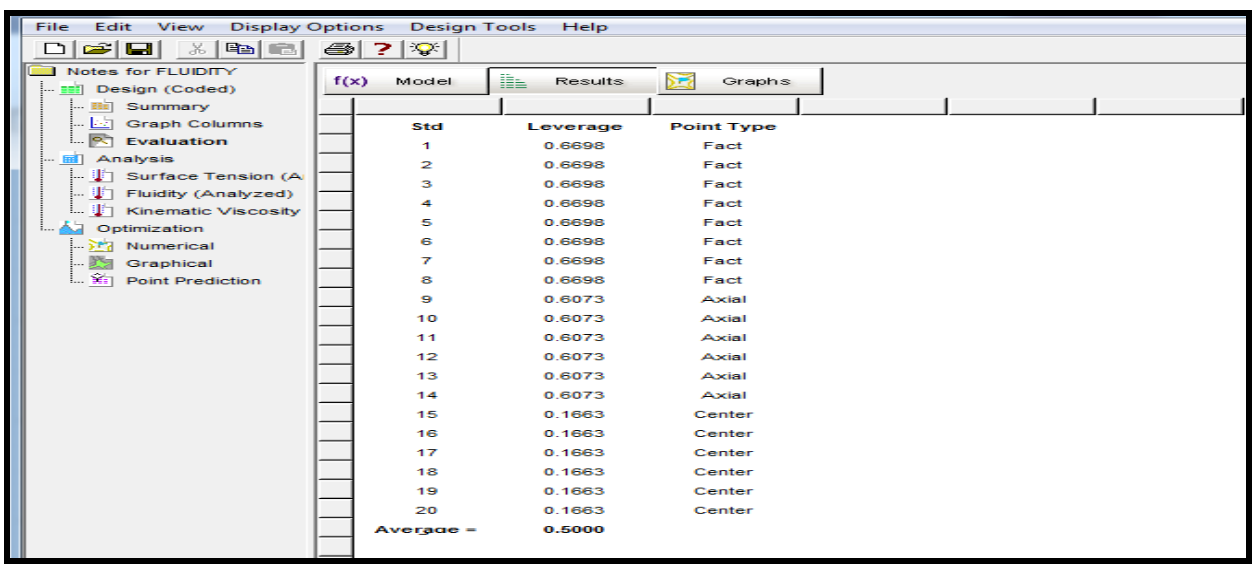

Std	Leverage	Point Type
1	0.6698	Fact
2	0.6698	Fact
3	0.6698	Fact
4	0.6698	Fact
5	0.6698	Fact
6	0.6698	Fact
7	0.6698	Fact
8	0.6698	Fact
9	0.6073	Axial
10	0.6073	Axial
11	0.6073	Axial
12	0.6073	Axial
13	0.6073	Axial
14	0.6073	Axial
15	0.1663	Center
16	0.1663	Center
17	0.1663	Center
18	0.1663	Center
19	0.1663	Center
20	0.1663	Center
Average =	0.5000	

Figure 12: Computed model leverages

Leverage of a point varies from 0 to 1 and indicates how much an individual design point influences the model's predicted values. A leverage of 1 means the predicted value at that particular case will exactly equal the observed value of the experiment, i.e., the residual will be 0. The sum of leverage values across all cases equals the number of coefficients (including the constant) fit by the model. The maximum leverage an experiment can have is 1/k, where k is the number of times the experiment was replicated.

In assessing the strength of the quadratic model towards maximizing the kinematic viscosity, one way analysis of variance (ANOVA) was done and result is presented in figure 13

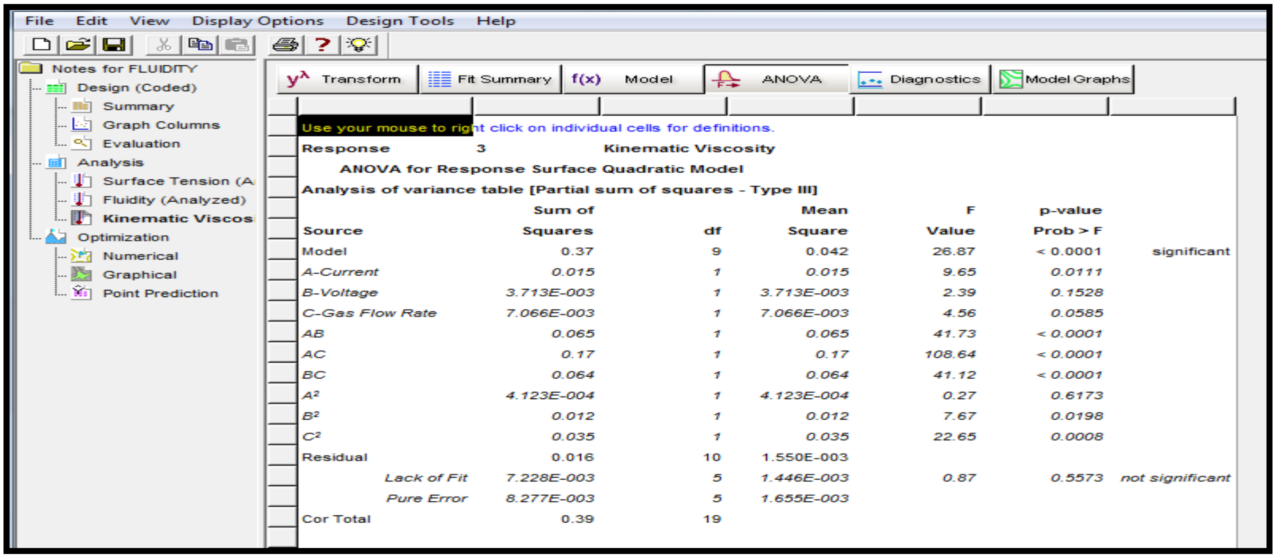

Source	Sum of Squares	df	Mean Square	F Value	p-value Prob > F	
Model	0.37	9	0.042	26.87	< 0.0001	significant
A-Current	0.015	1	0.015	9.65	0.0111	
B-Voltage	3.713E-003	1	3.713E-003	2.39	0.1528	
C-Gas Flow Rate	7.066E-003	1	7.066E-003	4.56	0.0585	
AB	0.065	1	0.065	41.73	< 0.0001	
AC	0.17	1	0.17	108.64	< 0.0001	
BC	0.064	1	0.064	41.12	< 0.0001	
A^2	4.123E-004	1	4.123E-004	0.27	0.6173	
B^2	0.012	1	0.012	7.67	0.0198	
C^2	0.035	1	0.035	22.65	0.0008	
Residual	0.016	10	1.550E-003			
Lack of Fit	7.228E-003	5	1.446E-003	0.87	0.5573	not significant
Pure Error	8.277E-003	5	1.655E-003			
Cor Total	0.39	19				

Figure 13: ANOVA table for validating the model significance towards maximizing the kinematic viscosity

Analysis of variance (ANOVA) was needed to check whether or not the model is significant and also to evaluate the significant contributions of each individual variable, the combined and quadratic effects towards each response.

From the result of figure 13, the Model F-value of 26.87 implies the model is significant. There is only a 0.01% chance that a "Model F-Value" this large could occur due to noise. Values of "Prob > F" less than 0.0500 indicate model terms are significant. In this case A, AB, AC, BC, B2, C2 are significant model terms. Values greater than 0.1000 indicate the model terms are not significant. The "Lack of Fit F-value" of 0.87 implies the Lack of Fit is not significant relative to the pure error. There is a 55.73% chance that a "Lack of Fit F-value" this large could occur due to noise. Non-significant lack of fit is good as it indicates a model that is significant.

To validate the adequacy of the quadratic model based on its ability to maximize the kinematic viscosity, the goodness of fit statistics presented in figure 14 were employed;

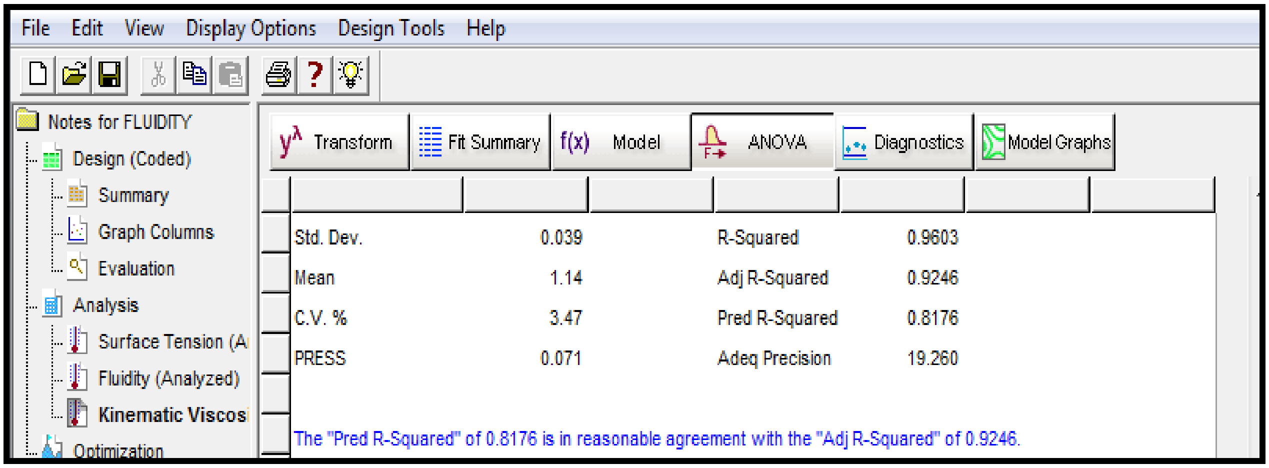

Std. Dev.	0.039	R-Squared	0.9603
Mean	1.14	Adj R-Squared	0.9246
C.V. %	3.47	Pred R-Squared	0.8176
PRESS	0.071	Adeq Precision	19.260

The "Pred R-Squared" of 0.8176 is in reasonable agreement with the "Adj R-Squared" of 0.9246.

Figure 14: GOF statistics for validating model significance towards maximizing the kinematic viscosity

From the result of figure 14 it was observed that the "Predicted R-Squared" value of 0.8176 is in reasonable agreement with the "Adj R-Squared" value of 0.9246. Adequate precision measures the signal to noise ratio. A ratio greater than 4 is desirable. The computed ratio of 19.260as observed in figure 14indicates an adequate signal. This model can be used to navigate the design space and maximize the kinematic viscosity

To obtain the optimal solution, we first consider the coefficient statistics and the corresponding standard errors. The computed standard error measures the difference between the experimental terms and the corresponding predicted terms. Coefficient statistics for kinematic viscosity is presented in figure 15

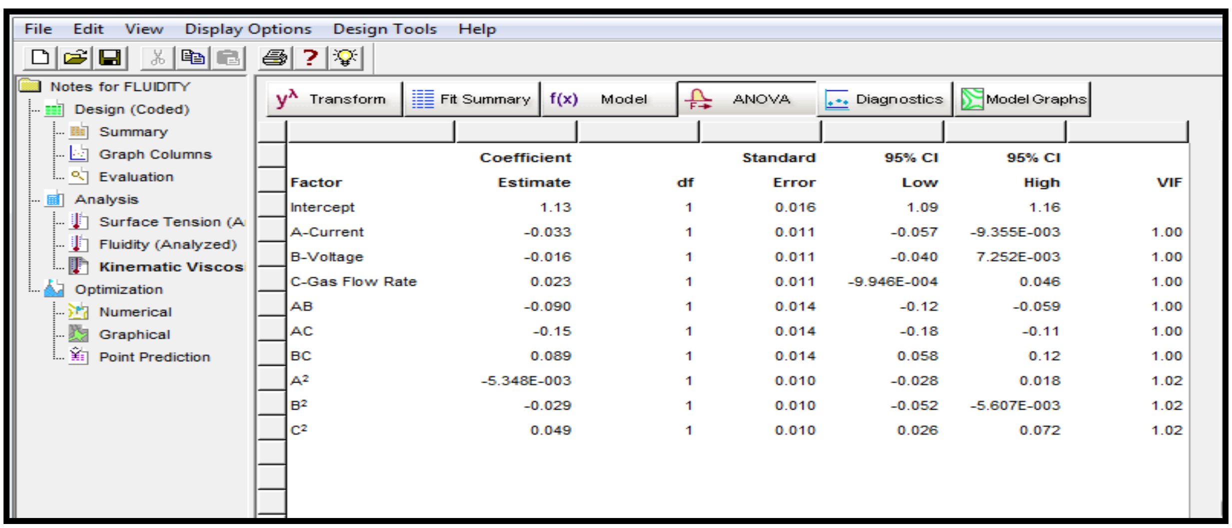

Factor	Coefficient Estimate	df	Standard Error	95% CI Low	95% CI High	VIF
Intercept	1.13	1	0.016	1.09	1.16	
A-Current	-0.033	1	0.011	-0.057	-9.355E-003	1.00
B-Voltage	-0.016	1	0.011	-0.040	7.252E-003	1.00
C-Gas Flow Rate	0.023	1	0.011	-9.946E-004	0.046	1.00
AB	-0.090	1	0.014	-0.12	-0.059	1.00
AC	-0.15	1	0.014	-0.18	-0.11	1.00
BC	0.089	1	0.014	0.058	0.12	1.00
A²	-5.348E-003	1	0.010	-0.028	0.018	1.02
B²	-0.029	1	0.010	-0.052	-5.607E-003	1.02
C²	0.049	1	0.010	0.026	0.072	1.02

Figure 15: Coefficient estimates statistics towards maximizing kinematic viscosity

Variance inflation factor (VIF) value of 1.00 for the individual and combine terms, 1.02 for the quadratic terms as observed in Table 15 indicate a significant model in which the variables are highly correlated with the responses.

The optimal equation which shows the individual effects and combines interactions of the selected input variables (current, voltage and gas flow rate) against the mesured responses (kinematic viscosity) is presented based on the coded variables in figure 16.

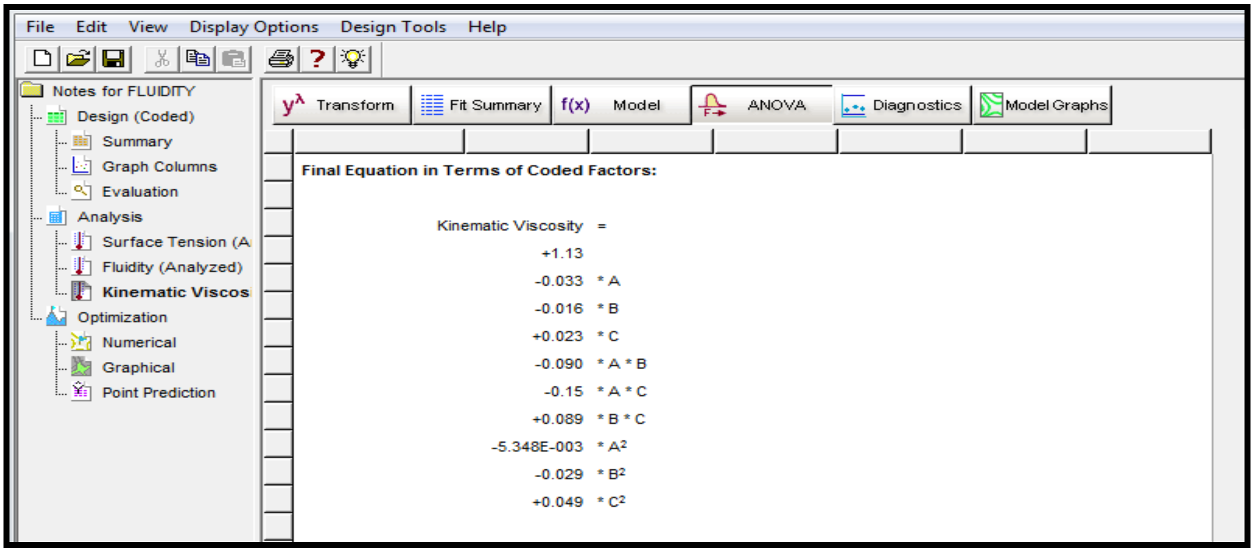

Figure 16: Optimal equation in terms of coded factors for maximizing kinematic viscosity

The optimal equation which shows the individual effects and combine interactions of the selected input variables (current, voltage and gas flow rate) against (kinematic viscosity is presented in actual factors in figure17

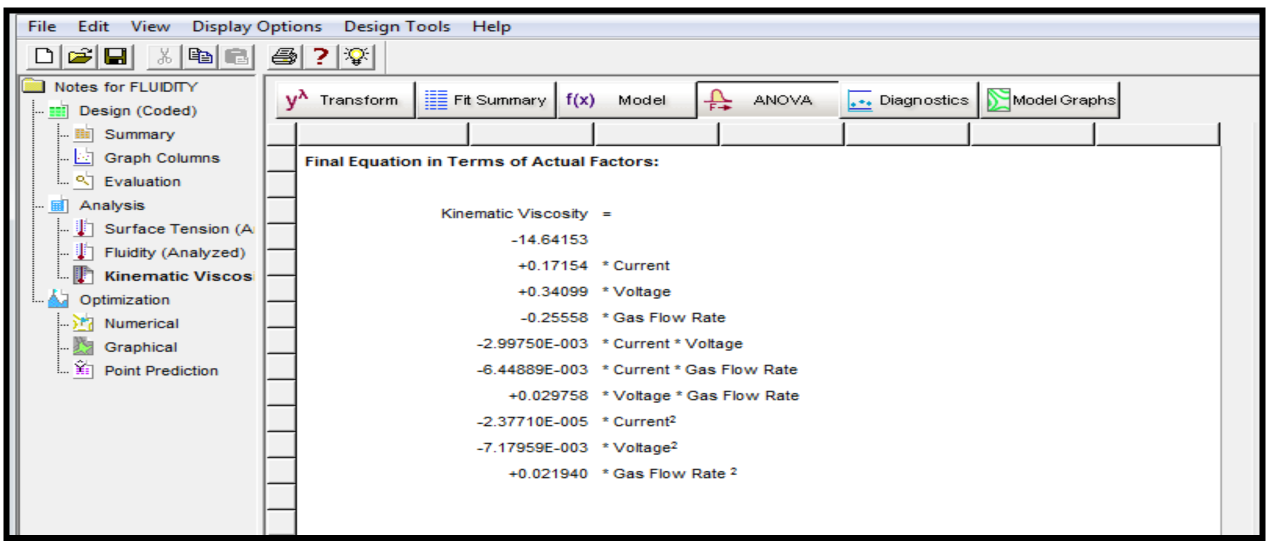

Figure 17: Optimal equation in terms of actual factors for maximizing kinematic viscosity

The diagnostics case statistics which shows the observed values of each respones variable (kinematic viscosity) against the predicted values is presented in figure 18. The diagnostic case statistics actually give insight into the model strength and the adequacy of the optimal second order polynomial equation.

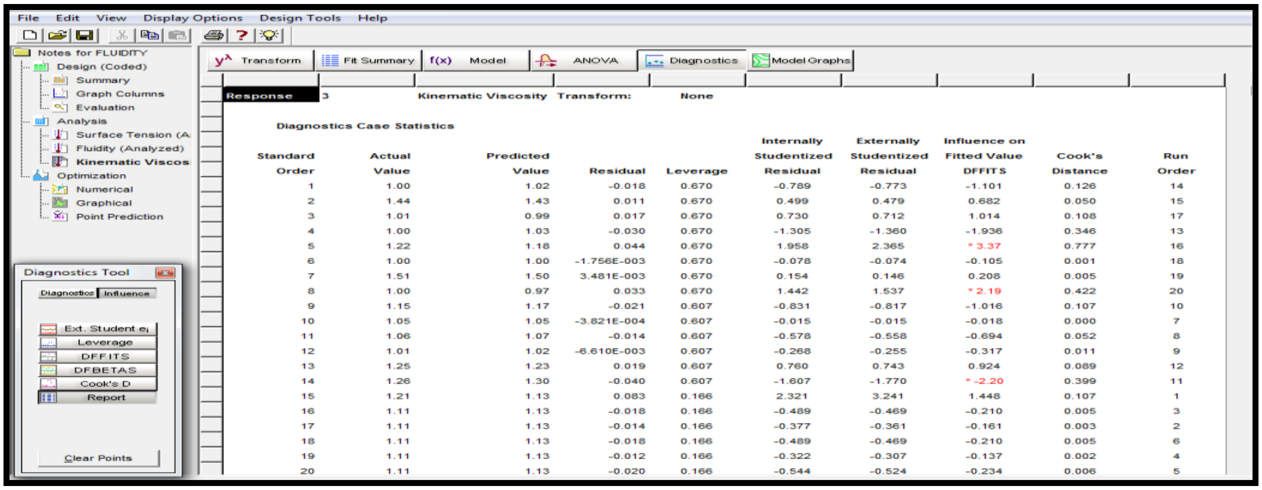

Response 3 Kinematic Viscosity Transform: None

Diagnostics Case Statistics

Standard Order	Actual Value	Predicted Value	Residual	Leverage	Internally Studentized Residual	Externally Studentized Residual	Influence on Fitted Value DFFITS	Cook's Distance	Run Order
1	1.00	1.02	-0.018	0.670	-0.789	-0.773	-1.101	0.126	14
2	1.44	1.43	0.011	0.670	0.499	0.479	0.682	0.050	15
3	1.01	0.99	0.017	0.670	0.730	0.712	1.014	0.108	17
4	1.00	1.03	-0.030	0.670	-1.305	-1.360	-1.936	0.346	13
5	1.22	1.18	0.044	0.670	1.958	2.365	* 3.37	0.777	16
6	1.00	1.00	-1.756E-003	0.670	-0.078	-0.074	-0.105	0.001	18
7	1.51	1.50	3.481E-003	0.670	0.154	0.146	0.208	0.005	19
8	1.00	0.97	0.033	0.670	1.442	1.537	* 2.19	0.422	20
9	1.15	1.17	-0.021	0.607	-0.831	-0.817	-1.016	0.107	10
10	1.05	1.05	-3.821E-004	0.607	-0.015	-0.015	-0.018	0.000	7
11	1.06	1.07	-0.014	0.607	-0.578	-0.558	-0.694	0.052	8
12	1.01	1.02	-6.610E-003	0.607	-0.268	-0.255	-0.317	0.011	9
13	1.25	1.23	0.019	0.607	0.760	0.743	0.924	0.089	12
14	1.26	1.30	-0.040	0.607	-1.607	-1.770	* -2.20	0.399	11
15	1.21	1.13	0.083	0.166	2.321	3.241	1.448	0.107	1
16	1.11	1.13	-0.018	0.166	-0.489	-0.469	-0.210	0.005	3
17	1.11	1.13	-0.014	0.166	-0.377	-0.361	-0.161	0.003	2
18	1.11	1.13	-0.018	0.166	-0.489	-0.469	-0.210	0.005	6
19	1.11	1.13	-0.012	0.166	-0.322	-0.307	-0.137	0.002	4
20	1.11	1.13	-0.020	0.166	-0.544	-0.524	-0.234	0.006	5

Figure 18: Diagnostics case statistics report of observed and predicted kinematic viscosity

Lower residual values resulting to higher leverages as observed in figure 18 are indicators of a well fitted model.

To assess the accuracy of prediction and established the suitability of response surface methodology using the quadratic model, a reliability plot of the observed and predicted values of kinematic viscosity was obtained as presented in Figures 19

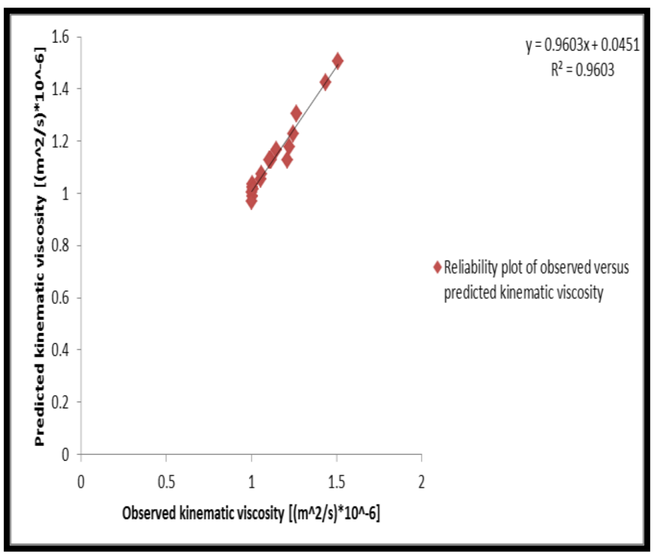

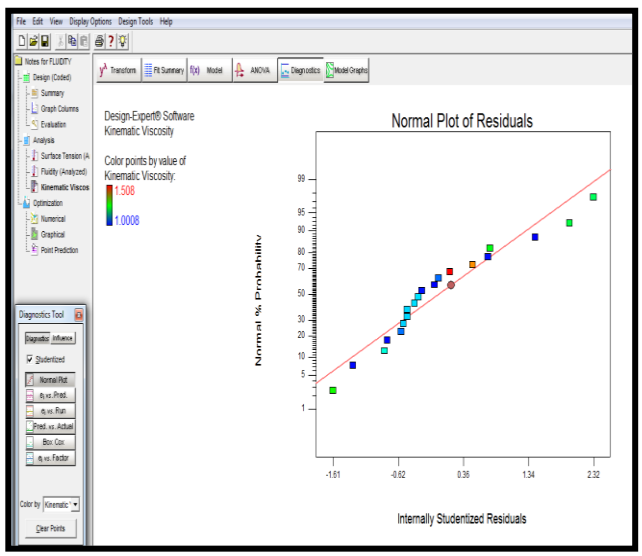

Figure 19: Reliability plot of observed versus predicted kinematic viscosity Figure 20: Normal probability plot of Student zed residuals for kinematic viscosity

The high coefficient of determination (r2 = 0.9288, 0, 9438 and 0.9603) as observed in Figure 19 were used to established the suitability of response surface methodology in maximizing the kinematic viscosity

To accept any model, its satisfactoriness must first be checked by an appropriate statistical analysis output. To diagnose the statistical properties of the kinematic viscosity model, the normal probability plot of residual presented in Figure 20

The normal probability plot of student zed residuals was employed to assess the normality of the calculated residuals. The normal probability plot of residuals which is the number of standard deviation of actual values based on the predicted values was employed to ascertain if the residuals (observed – predicted) follows a normal distribution. It is the most significant assumption for checking the sufficiency of a statistical model. Results of Figures 20 revealed that the computed residuals are approximately normally distributed an indication that the model developed is satisfactory and the data employed are devoid of possible outliers.

To determine the presence of a possible outlier, the cook's distance plot was generated for the kinematic viscosity. The cook's distance is a measure of how much the regression would change if the outlier is omitted from the analysis. A point that has a very high distance value relative to the other points may be an outlier and should be investigated. The generated cook's distance is presented in Figures 21

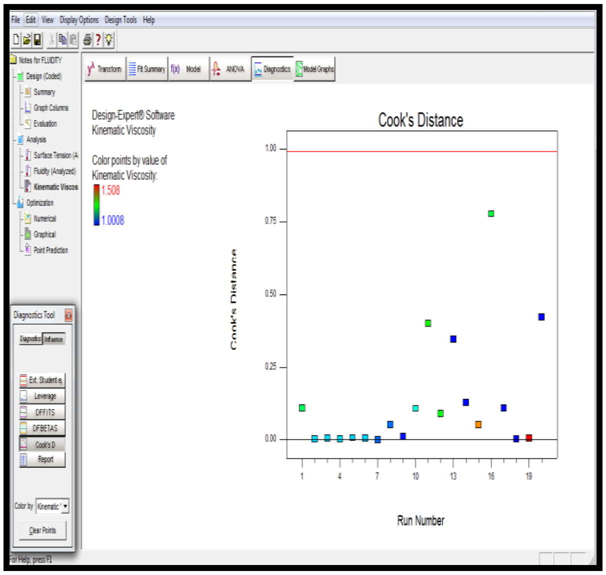

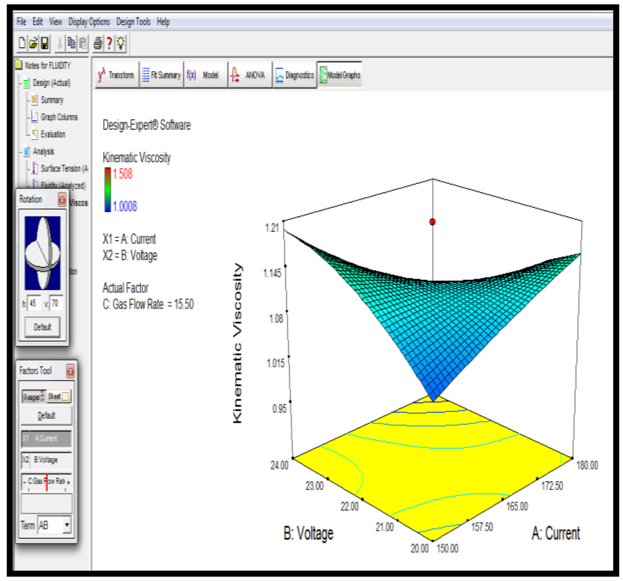

Figure 21: Generated cook's distance for kinematic viscosity Figure 22: Effect of current and voltage on kinematic viscosity

To study the effects of combine input variables on kinematic viscosity 3D surface plots is presented in Figure 22. The 3D surface plot as observed in Figure 22 shows the relationship between the input variables (current, voltage and gas flow rate) and the response variables (surface tension, fluidity and kinematic viscosity). It is a 3 dimensional surface plot which was employed to give a clearer concept of the response surface. Although not as useful as the contour plot for establishing responses values and coordinates, this view may provide a clearer view of the surface. As the colour of the curved surface gets darker, the surface tension decreases proportionately while the fluidity and kinematic viscosity increases. The presence of a coloured hole at the middle of the upper surface gave a clue that more points lightly shaded for easier identification fell below the surface.

Finally, numerical optimization was performed to ascertain the desirability of the overall model. In the numerical optimization phase, we ask design expert to; determine the optimum current (Amp), voltage (volts) and gas flow rate (L/min) that will maximize kinematic viscosity, The interphase of the numerical optimization showing the objective function is presented in Figure 23

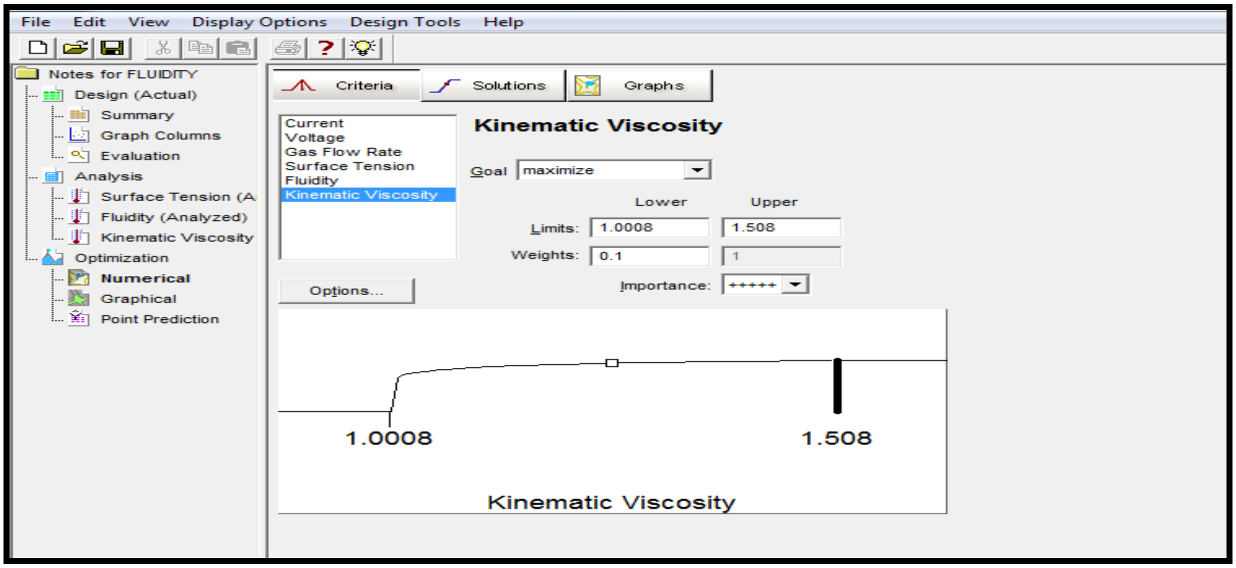

Figure 23: Interphase of numerical optimization model for maximizing kinematic viscosity

The constraint set for the numerical optimization algorithm is presented in figure 24.

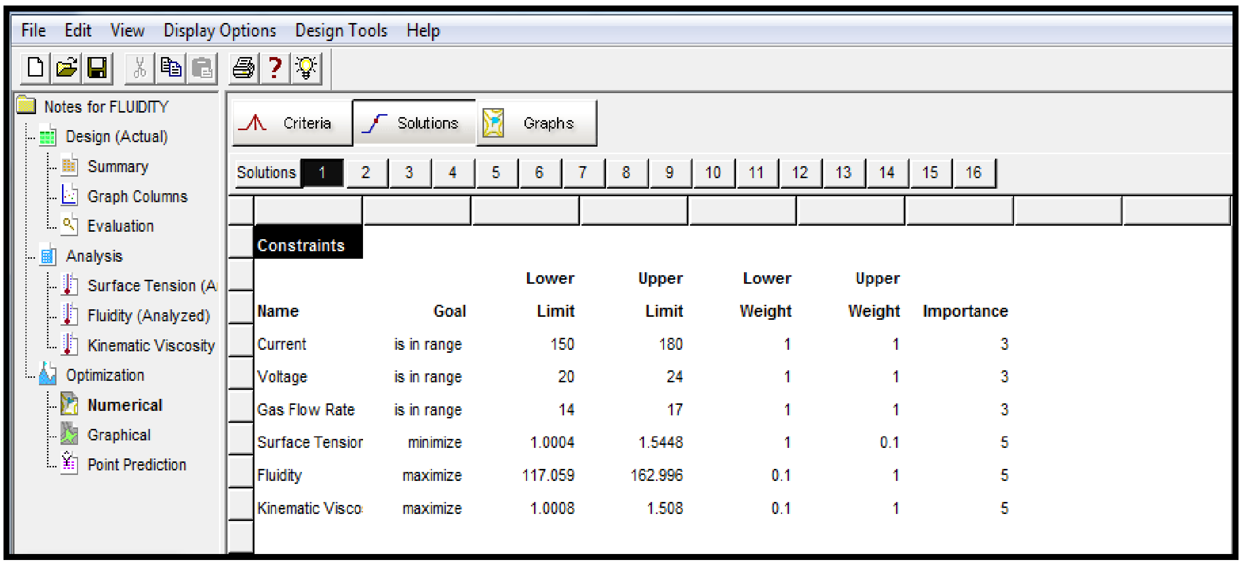

Name	Goal	Lower Limit	Upper Limit	Lower Weight	Upper Weight	Importance
Current	is in range	150	180	1	1	3
Voltage	is in range	20	24	1	1	3
Gas Flow Rate	is in range	14	17	1	1	3
Surface Tensior	minimize	1.0004	1.5448	1	0.1	5
Fluidity	maximize	117.059	162.996	0.1	1	5
Kinematic Visco	maximize	1.0008	1.508	0.1	1	5

Figure 24: Constraints for numerical optimization of selected responses

The numerical optimization generated about sixteen (16) optimal solutions which are presented in figure 25

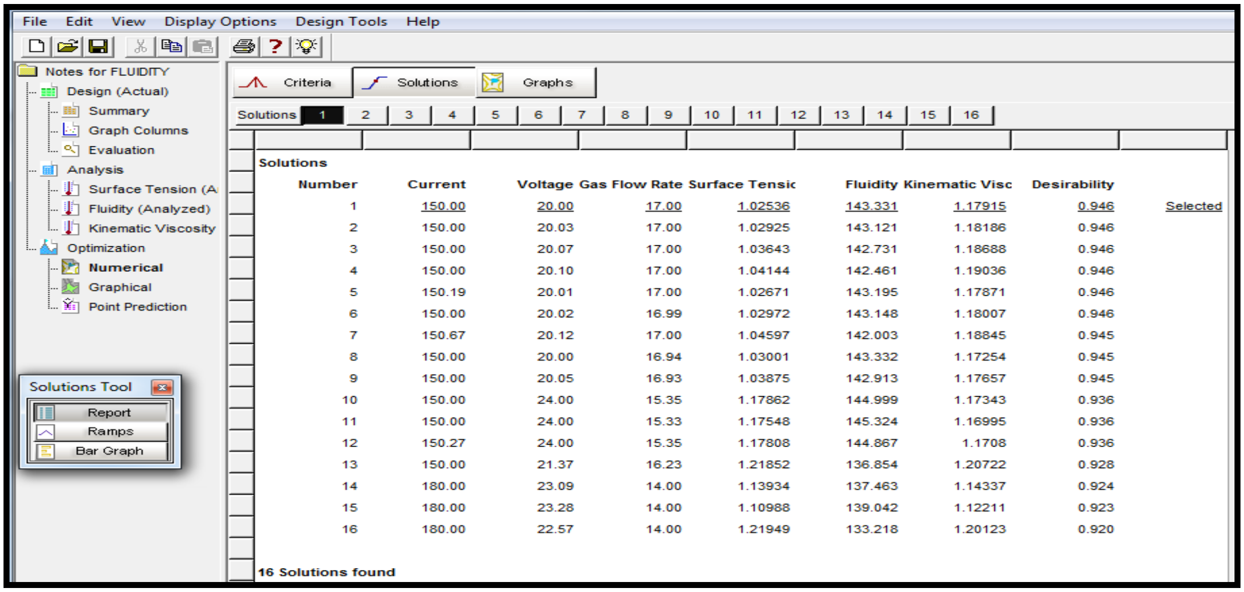

Number	Current	Voltage	Gas Flow Rate	Surface Tensic	Fluidity	Kinematic Visc	Desirability	
1	150.00	20.00	17.00	1.02536	143.331	1.17915	0.946	Selected
2	150.00	20.03	17.00	1.02925	143.121	1.18186	0.946	
3	150.00	20.07	17.00	1.03643	142.731	1.18688	0.946	
4	150.00	20.10	17.00	1.04144	142.461	1.19036	0.946	
5	150.19	20.01	17.00	1.02671	143.195	1.17871	0.946	
6	150.00	20.02	16.99	1.02972	143.148	1.18007	0.946	
7	150.67	20.12	17.00	1.04597	142.003	1.18845	0.945	
8	150.00	20.00	16.94	1.03001	143.332	1.17254	0.945	
9	150.00	20.05	16.93	1.03875	142.913	1.17657	0.945	
10	150.00	24.00	15.35	1.17862	144.999	1.17343	0.936	
11	150.00	24.00	15.33	1.17548	145.324	1.16995	0.936	
12	150.27	24.00	15.35	1.17808	144.867	1.1708	0.936	
13	150.00	21.37	16.23	1.21852	136.854	1.20722	0.928	
14	180.00	23.09	14.00	1.13934	137.463	1.14337	0.924	
15	180.00	23.28	14.00	1.10988	139.042	1.12211	0.923	
16	180.00	22.57	14.00	1.21949	133.218	1.20123	0.920	

Figure 25: Optimal solutions of numerical optimization model

From the results of Table 25, it was observed that a current of 150amp, voltage of 20volts and gas flow rate of 17.00L/min will produce a weld material with Kinematic Viscosity of 1.17915x10-6m2/s .This solution was selected by design expert as the optimal solution with a desirability value of 94.60%.

The desirability bar graph which shows the accuracy with which the model is able to predict the values of the selected input variables and the corresponding responses is presented in Figure 26.

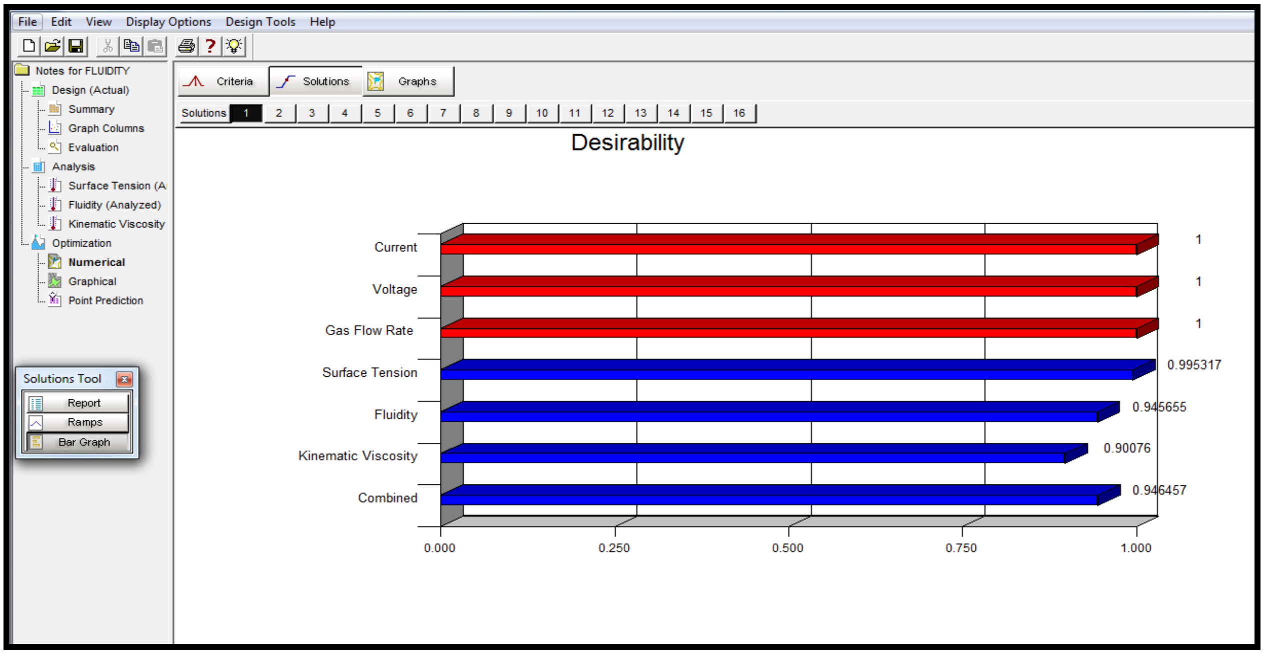

Figure 26: Prediction accuracy of numerical optimzation

It can be deduce from the result of Figure 4.52 that the model developed based on response surface methodology and optimized using numerical optimization method, predicted the Kinematic Viscosity with an accuracy level of 90.08%

The contour plots showing kinematic viscosity variable against the optimized value of the input variable is presented in Figure 27

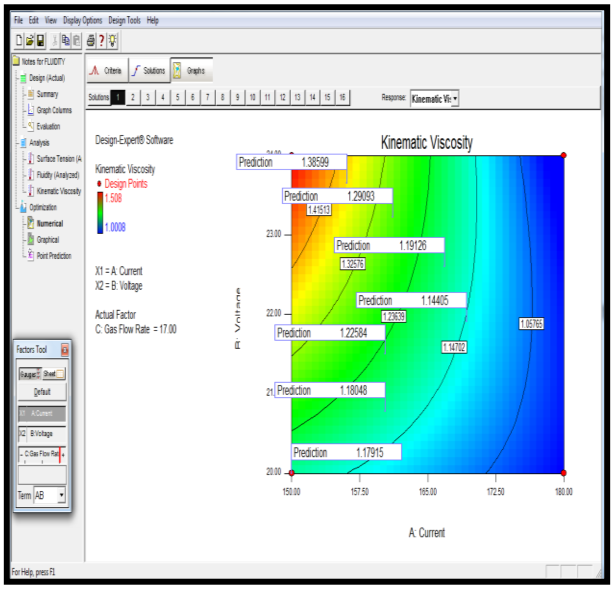

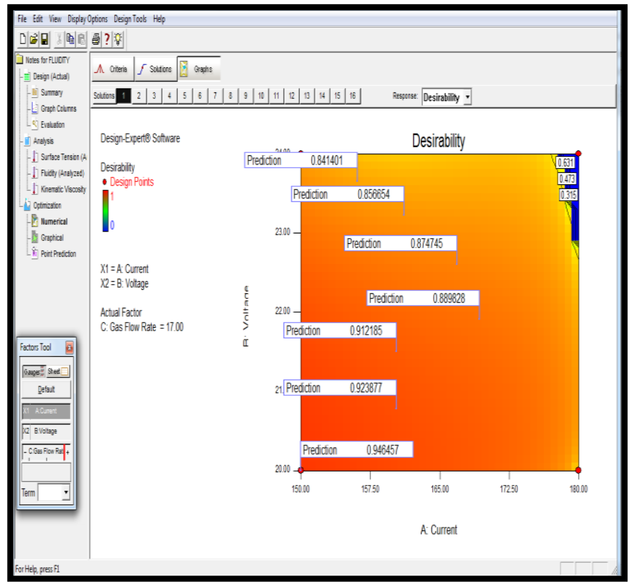

Figure 27: Predicting kinematic viscosity using contour plot Figure 28: Predicting desirability using contour plot

A plot of desirability against the input variables is presented in figure 28. As presented in Figures 28, the contour plot can be employed to predict the optimum values of the input variables based on the flagged response variables.

Conclusion

In this study, the response surface methodology was used to optimize the molten, metal properties such as Kinematic viscosity of gas tungsten arc mild steel welds. The Result revealed that the model is of the quadratic type which requires the polynomial analysis order as depicted by a typical response surface design. Coefficient of determination R2 values of 0.9603 kinematic viscosity model. Adeq Precision measures the signal to noise ratioof19.260which indicates adequate signal. From the results, it was observed that a current of 150.00 Amp, voltage of 20 volt and a gas flow rate of 17 L/min will produce a welded material having kinematic viscosity of 1.179 at a desirability of 0.946. Response surface methodology using numerical optimization was effective in predicting the kinematic viscosity.

Reference

Hildebrand, J.H. and Lamoreaux, R.H. (1976) Viscosity of Liquid Metals: An Interpretation Proc. Nat. Acad. Sci. USA, Vol. 73, No. 4, pp. 988-989.

Bakhtiyarov, S.I. and Over felt, R.A. (1999). Measurement of Liquid Metal Viscosity by Rotational Technique, Acta Metallurgica Inc. 47, (17); pp. 4311 – 4319.

Korolezuk-hjnank, M. and Migas, P. (2012) Analysis of Selected Liquid Steel Viscosity. Archives of Metallurgy and Materials, Vol. 57 Issue 4, pp. 963 – 969.

Kaptay, G. (2005) A Unified Equation For The Viscosity of Pure Liquid Metals. Z. Metallkd, 96 (1), pp. 1-8.

Boda, M.A., Bhasagi P.N., Sawade A.S., and Andodgi R.A. (2015) Analysis of Kinematic Viscosity for Liquids by Varying Temperature. International Journal of innovative Research in Science, Engineering and Technology, Vol. 4, Issue , pp. 1951 – 1954.

Ritwik (2012) Measuring the Viscous Flow Behaviour of Molten Metals Under Shear. Doctor of Philosophy Thesis. Brunel Centre For Advanced Solidfication Technology, Brunel University, United Kingdom.

Di Sabatino, M.; Amberg, L. And Apelian, D. (2008) Progress on the Understanding of Fluidity of Aluminium Foundry Alloys. International Journal of Metalcasting, Vol. 2, Issue 3, pp. 17-27.

Morando C, Fornaro O, Garbellini O and Palacio H (2015) "Fluidity on Metallic Eutectic Alloys" International Congress of Science and Technology of Metallurgy and Materials. Procedia Materials Science 8, pp. 959-967.

Davies, M.H. (1992) Numerical Modelling of Weld Pool Convection in Gas Metal Arc Welding. Doctor of Philosophy. Thesis. Department of Mechanical Engineering. The University of Adelaide, South Australia.

Achebo, J.I. (2012): Complex Behavior of Forces Influencing Molten Weld Metal Flow based on Static Force Balance Theory 2012 International Conference on Solid State Devices and Materials Science Physics Procedia 25 (2012) 317 – 324